Accepted for presentation in: European Wireless, Rome, Italy, October 2023.

IndoorDRaGon: Data-Driven 3D Radio Propagation Modeling for Highly Dynamic 6G Environments

Melina Geis[1], Hendrik Schippers[1], Marco Danger[1], Cedrik Krieger[1], Stefan Böcker[1], Julia Freytag[2], Irfan Fachrudin Priyanta[3], Moritz Roidl[3], and Christian Wietfeld[1]
[1]Communication Networks Institute, TU Dortmund University, 44227 Dortmund, Germany
[2]Fraunhofer-Institut for Material Flow and Logistics, 44227 Dortmund, Germany
[3]Chair of Material Handling and Warehousing, TU Dortmund University, 44227 Dortmund, Germany
e-mail:[1,3]{ Melina.Geis, Hendrik.Schippers, Marco.Danger, Cedrik.Krieger, Stefan.Boecker, IrfanFachrudin.Priyanta, Moritz.Roidl, Christian.Wietfeld}@tu-dortmund.de , [2]{Julia.Freytag}@iml.fraunhofer.de

***Abstract*—Private 5G and future 6G networks offer significant potential for automation in vertical domains but must face the challenge of dynamic and rapid adaptation to new operational requirements. In this context, non-stationary, ad-hoc network operation is essential for continuously adapting reliable network solutions to rapidly changing environments. In this paper, we present IndoorDRaGon as a novel signal-strength prediction method for network planning of dynamic environments that combines expert knowledge from the mobile communications domain with lightweight machine learning methods based on random forests to achieve accurate and computationally efficient spatiotemporal quality of service predictions. In a comprehensive performance evaluation, the performance of IndoorDRaGon is compared to real-world measurements, ray tracing analysis and a vast range of state-of-the-art channel models. It is found that IndoorDRaGon achieves significantly better accuracy for unseen environments than the latter, even when only a tiny portion of measurements is considered in the training data.**

***Video Abstract*—Video abstract can be accessed on http://tiny.cc/IndoorDRaGon**

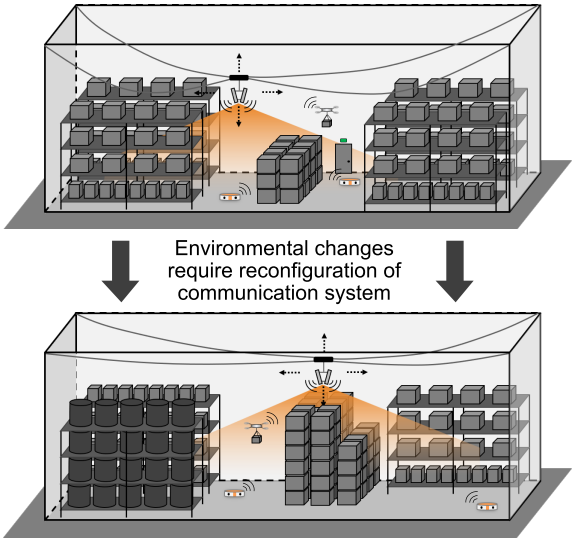

Fig. 1. Configurable 6G radio environment with flexible transmitter positions - enabled by the deployment of cable robots - to map dynamic scenarios that enable fully automated and modular manufacturing as well as intralogistics.

I. Introduction

Compared to preceding communication standards, the Fifth Generation of Mobile Communications (5G) is designed to serve a broader range of applications in various vertical domains, like industrial production, automotive, transportation, agriculture, and healthcare [1]. These applications can be divided into subgroups associated with special requirements and challenges. This variety of applications is likely to increase even further with the introduction of 6G.

Especially to fulfill the idea of Industry 4.0, that everything in automation is connected, 5G network infrastructures will be critical supporting assets [2]. The 3rd Generation Partnership Project (3GPP) defines some major challenges regarding communication networks for future factories in [3]. These include the demanding requirements of industrial-grade quality of service regarding low latency and reliability, the stringent requirements on safety, security and privacy, but also the need for high adaptability and scalability due to the multiple use cases and dynamic environments. Moreover, industrial radio propagation environments are characterized by very rich multipath and potentially high interference due to plenty of metallic objects and electrical machines.

That differs from most fields of applications that channel models are designed for, like public mobile networks in different outdoor environments. However, precise channel models are of key importance for planning and predicting wireless communications. However, the required detailed material-specific 3D models for indoor environments are usually lacking. Particularly in a dynamic environment, the existing models may be outdated, so new complex ray tracing calculations are necessitated.

A dynamic use case is shown in Fig. 1, where logistics robots are utilized for intralogistics applications. Based on the storage situation, shelf positions, and dimensions, the radio environment in the whole hall area changes. This effect is additionally superimposed on the competition for the transmission channel and the motion-induced change in the connection quality of each logistics robot entity. As the coverage of the private mobile network changes depending on the current storage configuration, re-configuring the base station location can be necessary and requires accurate channel modeling.

In this paper, we present IndoorDRaGon as a novel signal-

strength prediction method for complex 3D indoor environments encountered in industrial use-cases. IndoorDRaGon utilizes environmental information of existing 3D indoor models by calculating sectional planes based on its predecessor Deep RAdio channel modeling from GeOinformatioN (DRaGon) [4] and extracts numerical features from these based on the idea of TinyDRaGon [5]. The intralogistics use case in Fig. 1 is one example that benefits from IndoorDRaGon, as the changing connectivity situation in the whole area can be closely replicated by IndoorDRaGon channel predictions. For feasibility reasons, only two static antenna positions are considered.

The remainder of the paper is structured as follows. After discussing the related work in Sec. II, we present the novel IndoorDRaGon method in Sec. III. Afterwards, an overview of the methodological aspects is given in Sec. IV. Detailed results are provided and discussed in Sec. V and Sec. VI.

II. Related Work

Empirical studies on channel models have been widely used in past research. Modeling complexity differs from purely distance-based models [6], over comprehensive studies [7][8], to yield scenario-specific definitions, up to numerical methods like ray tracing [9], where the physical behavior of individual rays is modeled and simulated. Although such approaches attempt to respect the environment in fine granularity, the price of high computational cost does not eliminate the prediction error for specific scenarios.

In previous works [4], [5], we presented DRaGon and its lightweight successor TinyDRaGon. There, empirical measurements for training Machine Learning (ML)-based algorithms were utilized and have shown to overcome conventional models as well as methods like ray tracing regarding prediction error and computational cost for outdoor scenarios. Two image samples are taken into account, one showing the direct paths' side view and one showing the top view of the receivers surrounding area. To do so, different geological databases were considered in order to model buildings and terrain. In TinyDRaGon, these images are eliminated by extracting numerical features based on the number of non-white pixels. In [14], it is found that ML can be effectively used for path loss estimation in indoor office environments. To overcome poor prediction accuracy when only one model for all environments is utilized, the authors of [15] propose a dynamic indoor channel model based on a cluster identification algorithm.

TABLE I
Overview of Channel Modeling Methods and their Properties.

Method	Properties			
	Pos.	Obstacles	Mat.	Type
Friis [6]	◑	○	○	AM
ABG [10]	◑	○	○	EF
3GPP Indoor InH / InF [7]	◑	◑	○	EM
WINNER II (A1 / B3) [11]	●	●	◑	env.-aw. EM
Ray Tracing [9]	●	●	●	env.-aw. PM
ABG + WL [12], [13]	●	●	●	env.-aw. EF
Proposal: IndoorDRaGon	●	●	■	**env.-aw. ML**

Legend: ● - Explicit Modeling, ◑ - Abstract Consideration, ○ - Unconsidered, ■: IndoorDRaGon learns materials implicitly during training, minimizing the modeling effort.
AM - Analytical Model, **EF** - Empirical Fit, **EM** - Empirical Model, **PM** - Physical Model, **env.-aw.** - environment-aware

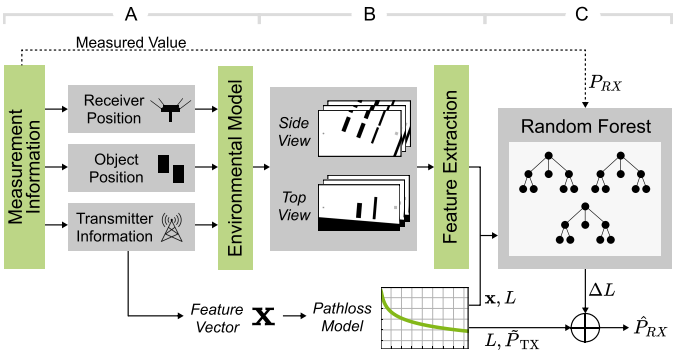

Fig. 2. System architecture model of the proposed IndoorDRaGon received power prediction method.

We extensively studied existing channel modeling methods, which we present in Tab. I. Conventional models usually do not consider properties like **position**, **obstacles**, or **materials** at all, or as an abstract parameter such as a distance value in the case of position information or probabilistic modeling of the Line-of-Sight (LOS) condition [7]. They differ in their **type**, being either analytical or empirical, which is further distinguished into models, empirically fitted to the environment, and general empirical models. Other models add the component of environmental awareness and explicitly model positions and obstacles. WINNER II (A1/B3) [11] supports an abstract consideration of floor and wall loss (WL), whereas advanced methods like ray tracing [9] aim to numerically calculate radio propagation based on physical models. Based on an Alpha-Beta-Gamma (ABG) model [10], the authors of [13] present a model for the Radio Environmental Map (REM) calculation of indoor factory halls together with an additional WL according to [12]. We refer to this kind of model as ABG + WL. Our proposal IndoorDRaGon on the other hand is based on ML as explained in Sec. III.

III. Machine Learning Approach

Problem Statement: Our goal is to retrieve a model for the calculation of the Received Signal Strength (RSS) at a specific receiver position $\mathbf{p}_{\mathrm{RX}}$ given the transmitter position $\mathbf{p}_{\mathrm{TX}}$ in an indoor environment. We utilize a generic model

$$P_{\mathrm{RX}}(\mathbf{p}_{\mathrm{RX}}, \mathbf{p}_{\mathrm{TX}}) = \underbrace{\tilde{P}_{\mathrm{TX}}}_{\substack{\text{Communication}\\ \text{system}}} - \underbrace{L(\mathbf{p}_{\mathrm{RX}}, \mathbf{p}_{\mathrm{TX}})}_{\substack{\text{Channel}\\ \text{model}}} + \underbrace{\Delta L(\mathbf{x})}_{\substack{\text{ML-based}\\ \text{correction}}} \quad (1)$$

that estimates P_{RX} based on $\tilde{P}_{\mathrm{TX}}$, the path loss of an analytical radio channel model L, and a correction offset ΔL. $\tilde{P}_{\mathrm{TX}}$ accumulates the transmit power as well as the antenna gains and losses of receiver and transmitter. We rely on free space propagation for determining L. Finally, ΔL is obtained using the proposed ML pipeline processing the information in the feature vector x. The ML model is designed to accurately predict ΔL by learning the wave propagation in a specific logistics hall and the effects of objects and their arrangements

in the three-dimensional space. The overall system architecture model of the proposed IndoorDRaGon can be seen in Fig. 2.

Data Preprocessing: Since our previous works DRaGon [4], and TinyDRaGon [5] yield high channel prediction accuracy by using synthetic images of the receiver's top-view and side-view, we employ a similar procedure for the proposed IndoorDRaGon model. To retrieve analogous synthetic images for an indoor environment, three-dimensional modeling of the scenario of interest is required. However, to create this, detailed information about the environment is indispensable, which, compared to outdoor environments, is generally not open-source available, but in many cases covered by existing Digital Twins (DTs) (cf. Fig. 2 A).

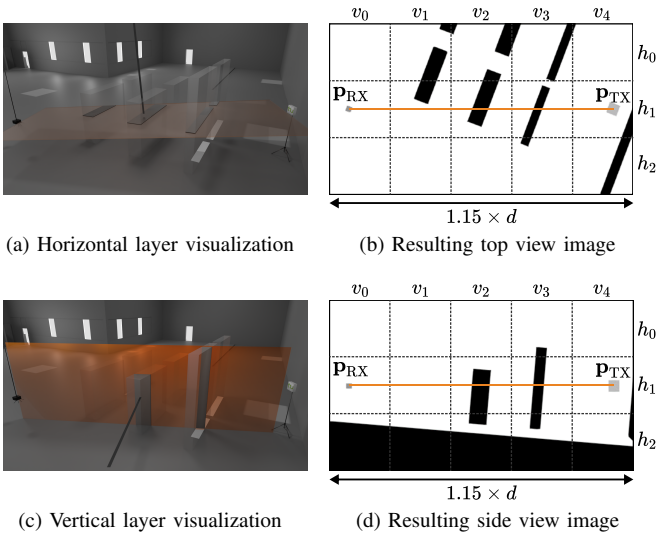

(a) Horizontal layer visualization (b) Resulting top view image

(c) Vertical layer visualization (d) Resulting side view image

Fig. 3. Feature Extraction (cf. Fig. 2 B): Illustration of automatic cut layer creation for *hallway scenario 2* (cf. Fig. 4). The intersection of the layer with obstacles is rendered from the normal direction in the middle between the transmitter and receiver. Following, mathematical features from the resulting images are extracted (cf. Tab. II). Note that h_i indicates a horizontal and v_i a vertical split.

For the side-view perspective, a vertical cut is used by defining the cut plane by a second vector orthogonal to the ground plane. The first image sample shows the receiver's and transmitter's direct path from a slightly tilted top-view perspective, as the height difference between transmitter and receiver is non-zero in general. Therefore, two three-dimensional planes are created based on the vector passing through the receiver's and transmitter's positions, as illustrated in Fig. 3 (a) and (c). For each transmitter-receiver pair, two image samples are created showing the environment's "horizontal" and "vertical" cuts. Consequently, the intersections of the scenario model with these planes are then extracted as images, where black indicates an obstacle and white indicates empty space (see Fig. 3 (b) and (d)). Thereby, we implicitly incorporate height information of the objects and the ceiling height. The depicted area is in $16 : 9$ format. The horizontal range is based on the transmitter-receiver distance d, so the transmitter and the receiver always occur at the same position in the resulting image. The covered range is chosen as $1.15 \times d$.

TABLE II
LOGICAL DOMAINS OF UTILIZED ML FEATURES.

Domain	Features
$\mathbf{x}_{\text{com}}$	Carrier frequency f, bandwidth B, transmission power P_{TX}, estimated path loss L
$\mathbf{x}_{\text{pos}}$	Position differences Δx, Δy, Δz, deviation from main antenna beam $\Delta\vartheta$, $\Delta\varphi$, 2D and 3D distance d_{2D}, d_{3D}
$\mathbf{x}_{\text{img}}$	Relation of obstacle pixels for three horizontal and five vertical split sections for top-view ($\mathbf{x}_{\text{top}}$) and side-view ($\mathbf{x}_{\text{side}}$) images
$\mathbf{x}_{\text{env}}$	oLOS distance d_{OLOS}, number of intersections N_{IS}

The images, as such, are eliminated in the following by extracting numerical features directly from them. During this process, both image types are split into equally sized Regions of Interest (RoIs) for which the ratio between obstacle pixels and overall pixels is computed. The splits are performed in such a way that three horizontal $h_0, ..., h_2$ and five vertical $v_0, ..., v_4$ RoIs are created. A visualization of the latter can be seen in Fig. 3 (b) and (d). Also, based on the extracted images, direct path information regarding the obstructed LOS (oLOS) distance, meaning the distance traveling through obstacles, and the number of intersections with obstacles is extracted.

Further, various features are derived based on the transmitter information, including the 3D position $(x_{\text{TX}}, y_{\text{TX}}, z_{\text{TX}})$, the carrier frequency f, the bandwidth B, the transmit power P_{TX}, and the main beam direction's elevation and azimuth angle (ϑ, φ) as well as the receiver's 3D position $(x_{\text{RX}}, y_{\text{RX}}, z_{\text{RX}})$. For the feature vector, we use delta values of x, y, and z coordinates of the transmitter and receiver locations. In addition, we include the difference of angles between the antenna's direct path and the main beam direction, namely $(\Delta\vartheta, \Delta\varphi)$. Moreover, expert knowledge is incorporated by calculating an estimate of the path-loss L_{PL} based on the free space propagation model.

Data Analysis: The resulting overall feature vector holds 29 variables from different logical domains shown in Tab. II. For the actual ML processes, the scikit-learn toolkit for python is utilized. Based on the results in [5], we apply Random Forests (RFs) [16] with improved interpretability compared to other ML algorithms (cf. Fig. 2 C). RFs are ensemble methods that derive a so-called strong learner by combining different uncorrelated decision trees, where each tree only considers a subset of the measurements and features. Although RFs do not tend to overfit, tuning the hyperparameters can improve the model's performance. Therefore, we perform a random search on the aggregated measurement dataset to find an optimized hyperparameter configuration regarding the number of decision trees, the maximum depth per tree, the minimum number of samples required to be at a leaf node, and the minimum number of samples required to split an internal node.

IV. VALIDATION METHODOLOGY

Measurement Scenarios: The Innovationlab research hall of the Chair of Material Handling and Warehousing (FLW)

of the TU Dortmund university [17] is a modern logistic warehouse testbed used for the experiments conducted in this work. The implemented Motion Capture System (MoCap) in the FLW research hall acts as an optical reference system for localization-based research with sub-mm accuracy. The MoCap system localizes objects within a capture distance of approximately 5 to 6 meters, by tracking retro-reflective markers attached to the object. A 3-axis cable robot system, geared with a modem, is intended to perform 3D radio frequency mapping in our experiment scenarios. The robot platform is attached to four winches placed in the four upper corners of the research hall. Within a 198 m^2 safety zone, it can maneuver to any position according to a given trajectory and speed input.

In the hall, we capture multiple indoor logistics scenarios with radio-reflective materials. These reflective materials symbolize typical warehousing environments with metallic shelves containing objects that interfere with the radio signals. Despite one empty scenario, each scenario consists of eight heavy-duty shelves connected in pairs, such that we have four double shelves with 2.05 m width, 2.0 m height, and 0.535 m depth. Further, the scenarios contain two folding displays, each with 2.27 m width, 3.02 m height, and 0.29 m depth. We defined six distinct measurement scenarios, as visualized in Fig. 4, to model a dynamic intralogistics environment. We decided to use an aluminum vapor barrier membrane in our scenarios, which is used to cover the barriers, as it is comparably robust, lightweight and easy to handle (see Fig. 5 (b)).

Data Collection: We utilized a 5G campus network with one antenna placed in the hall. The network parameters are shown in Tab. III. A transmission power of 0 dBm was chosen to include cell center and cell edge effects in the measurement area. A 5G capable modem, see Fig. 5 (a), with four antennas, is connected to a powerful Single Board Computer (SBC), which is connected to the optical localization system via an additional Ethernet interface. On the SBC, repeated signal strength and quality measurements are triggered to get a three-dimensional REM while the cable robot traverses through the hall.

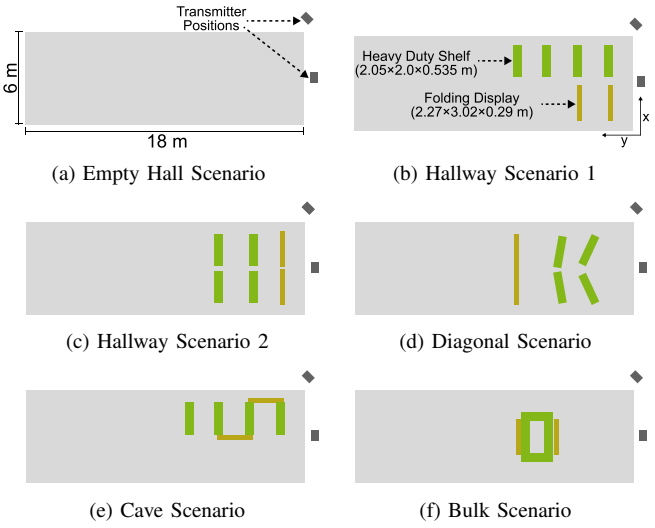

(a) Empty Hall Scenario (b) Hallway Scenario 1

(c) Hallway Scenario 2 (d) Diagonal Scenario

(e) Cave Scenario (f) Bulk Scenario

Fig. 4. Scenario top-views for the measurement of three-dimensional connectivity maps.

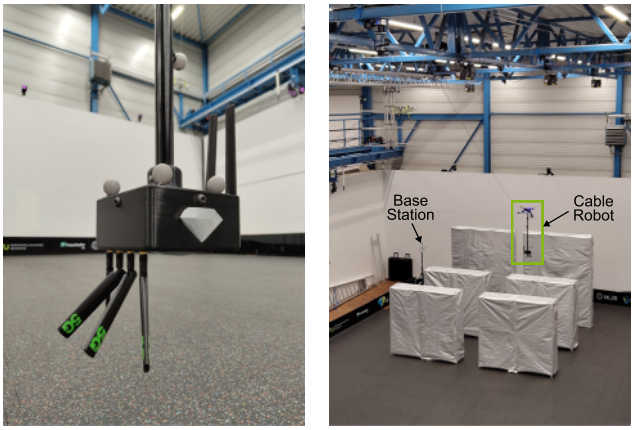

(a) Cellular private network modem utilized for data collection (b) Measurement setup for *hallway scenario 2*

Fig. 5. Utilization of the developed measurement box attached to the cable robot.

First, we created measurements in the empty hall by traversing it grid-based with the cable robot. For this, we use a grid resolution of 1 m, which results in 182 456 measurements. These measurements are transferred into a three-dimensional map by voxelization with a width of 0.2 m to increase the measurement accuracy of each sample (see Fig. 6). By averaging over multiple measurements, potential noise is decreased. This way, the number of measurement points is reduced to slightly over 2 000 per scenario. After the three-dimensional measurement of the entire hall, the measurement scenario was changed as planned. Then, the same measurement process was repeated but with an adapted grid size of 2 m to ensure safety distances to obstacles. For the six measurement scenarios, we contained two different antenna locations for each scenario (see Fig. 4 (a)). One is horizontally centered at the shorter wall pointing in the normal direction of the wall, and one antenna location is set to be at the corner of the hall with a tilt of 45 degrees.

TABLE III
UTILIZED 5G CELL PARAMETERS FOR THE MEASUREMENT CAMPAIGN.

Parameter	**Value**
Center Frequency	3725 MHz
Bandwidth	50 MHz
Subcarrier Spacing	30 kHz
Transmission Power	0 dBm
TDD Pattern	5:5

A simplified 3D model based on the DT is then loaded in an open source 3D software (Blender) and enriched with the obstacles corresponding to the measurement scenario. The image generation, as described in Sec. III, is then performed by rendering section planes through the transmitter and receiver for each measurement. The resulting dataset contains 27,472 samples.

Validation Methods: In order to validate the IndoorDRaGon model, it is later compared to multiple path loss prediction models from various categories:

- *Analytical models* such as Friis [6]
- *Empirical models* such as 3GPP Indoor Factory (InF) [7] and WINNER II B3 [11]
- *Empirically fitted models* with optional added material-specific environmental awareness such as ABG model and ABG + WL [13]
- *Physical models* with environmental awareness such as ray tracing

As given in Eq. 1, P_{RX} depends on $\tilde{P}_{\mathrm{TX}}$ that aggregates transmission power, antenna gains and coupling losses. We use the free space loss [6] to estimate $\tilde{P}_{\mathrm{TX}}$ based on the measurements in the empty hall scenario with $\mathbf{p}_{\mathrm{TX1}}$, which are located close to the main antenna beam: $|\Delta x| \leq 0.5\,\mathrm{m}$ and $|\Delta z| \leq 0.5\,\mathrm{m}$. For that purpose, the measured Reference Signal Received Power (RSRP) values are first converted into the received power P_{RX} using the following formula according to [18]:

$$\mathrm{RSRP} = P_{\mathrm{RX}} - 10\log_{10}(N_{\mathrm{RB}} \cdot N_{\mathrm{SC}}) \tag{2}$$

where N_{RB} is the number of Resource Blocks (RBs), determined by the bandwidth and the Subcarrier (SC) spacing [19], and N_{SC} is the number of SCs, which is fixed to 12. Further, the parameters of the ABG model and the WL model utilized in [13] are fitted on the measured values close to the direct antenna beam by performing a simple regression.

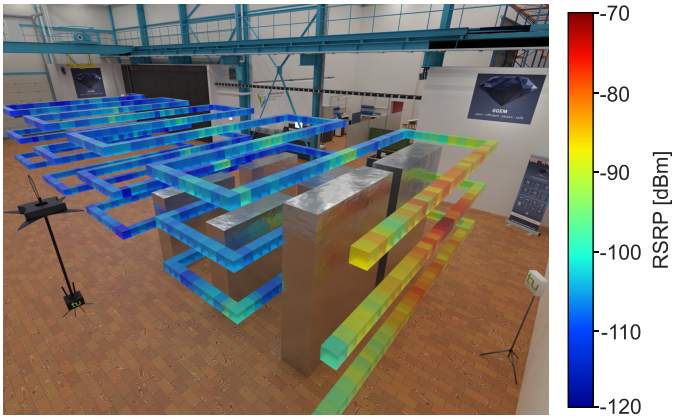

Fig. 6. Measured RSRP distribution of the hall in the digital twin for the *hallway scenario 2*. The visualized data is collected by traversing the cable-robot grid-wise in three different height layers.

V. Performance Comparison

As a performance comparison, the Empirical Cumulative Distribution Function (ECDF) of the absolute prediction error of the proposed IndoorDRaGon model and the reference models, listed in Sec. IV, is shown in Fig. 7. For this purpose, the RF is trained on 80% of the aggregated and shuffled measurement samples. Based on the hyperparameter tuning, we use 50 decision trees with a maximum depth of 30. Further, we use a minimum number of five samples to split an internal node, a minimum number of two samples required to be at

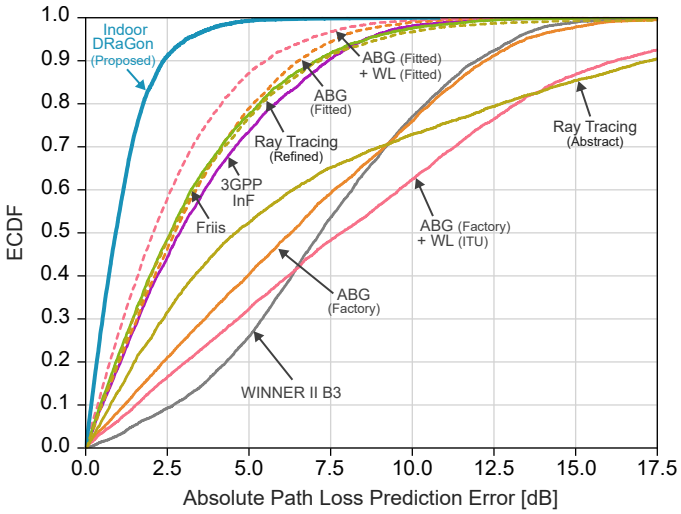

Fig. 7. Comparison of the absolute path loss prediction errors of IndoorDRaGon and other benchmarks, defined in Tab. I, evaluated on the measurement data.

a leaf node, enabled bootstrapping, and $\sqrt{29}$ as the number of features to consider when looking for the best split. The remaining 20% of measurement data, which consists of $5{,}494$ samples, is used to evaluate IndoorDRaGon as well as the reference models. Hereby, the training with only one CPU kernel takes $14.89\,\mathrm{s}$, while testing takes $0.05\,\mathrm{s}$.

The IndoorDRaGon model outperforms all models with a prediction error of $1.55\,\mathrm{dB}$ Root Mean Square Error (RMSE). Among the models that have not been given any information on the measurement data, the analytical and empirical channel models that lack environmental information achieve RMSE values of $4.22\,\mathrm{dB}$ for Friis free space propagation, $4.42\,\mathrm{dB}$ for the 3GPP InF model, and $8.11\,\mathrm{dB}$ for the WINNER II B3 model. *Factory* ABG refers to parameterization from [13], where the utilized data was collected in a factory environment, and achieves $7.82\,\mathrm{dB}$ prediction RMSE. Adding standard WL parameterization for metallic surfaces by *ITU* [12] leads to the worst accuracy with an RMSE of $10.26\,\mathrm{dB}$. By taking a closer look at the data, it is revealed that the aforementioned models are too pessimistic, as the measured RSRP values do not decrease so heavily with the distance as assumed by the models. Utilizing a small amount of measurement data for curve fitting the ABG parameters and WL parameters improves the prediction error to $3.98\,\mathrm{dB}$ and $3.33\,\mathrm{dB}$ RMSE, respectively. *Fitted* version of ABG + WL raises it to the second best performance behind IndoorDRaGon, which emphasizes the importance of a scenario-specific model parameterization.

The physical model using ray tracing is also evaluated in two subsequent steps. First, we see that the ray tracing simulation with an *abstract* model of the environment performs poorly with an RMSE of $9.30\,\mathrm{dB}$. Consequently, we add a higher grade of details to the model, by optimizing the material and object properties within our environment. We refer to this as *refined* ray tracing, improving to an RMSE of $4.30\,\mathrm{dB}$. On the one hand, this shows the high potential of ray tracing if all necessary information about the environment is available,

but, on the other hand, the high effort demanded to produce accurate results. The key advantages of IndoorDRaGon are its ability to achieve precise results even with a simplified environment model, with which ray tracing underperforms, and its ability to respond quickly to volatile environments.

VI. Generalization Capability Analysis

As it is not always feasible to conduct exhaustive measurement campaigns, the following section analyzes how a limitation of the measurement samples affects IndoorDRaGon's prediction accuracy. Therefore, we compare different data aggregation approaches:

- **Local:** an individual split evaluation is done for each scenario, so that 80 % of the shuffled data is used for training and remaining 20 % for testing.
- **Global:** the model is trained using a subset of all scenarios, meaning that 80 % of the aggregated and shuffled data is utilized for training.
- **Cross-scenario:** the data samples originating from the scenario under investigation are used for testing, while all data samples from the remaining scenarios are used for training.

The results on *hallway scenario 1* are visualized as a boxplot in Fig. 8. It can be seen that the local approach yields the best results with a prediction error of 1.47 dB RMSE. The global approach has a similar performance with 1.52 dB. Next, we consider the cross-scenario approach on all remaining scenarios, where IndoorDRaGon achieves 2.14 dB RMSE. For reference, the fitted ABG + WL achieves an RMSE of 3.21 dB. This demonstrates IndoorDRaGon's capability to provide accurate predictions even on unseen scenarios. To further investigate this transferability, we trained the model on *hallway scenario 2* and tested it on the similar *hallway scenario 1*, named here **cross-hallway 2**. Although the amount of training data is highly limited, IndoorDRaGon achieves prediction accuracy of 1.95 dB RMSE indicating that training on all scenarios instead of one similar scenario complicates the prediction task.

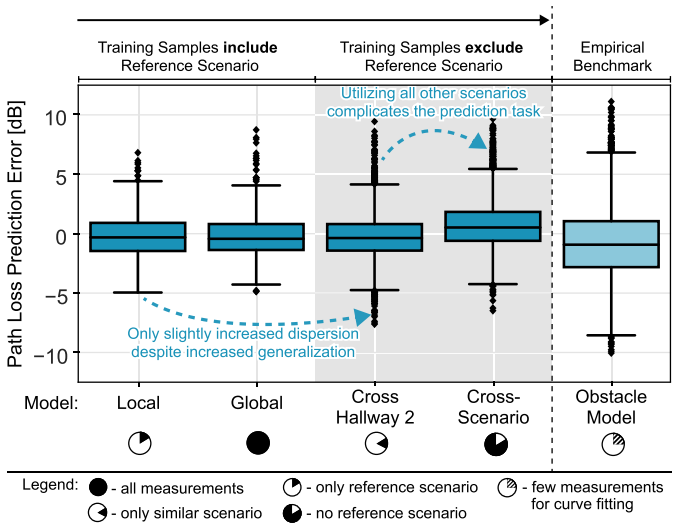

Fig. 8. Comparison of IndoorDRaGon's prediction accuracy evaluated on a hold out set of *hallway scenario 1* for different data aggregation methods.

The prediction RMSE values over the several models for all scenarios are listed in Tab. IV. In addition, the achieved prediction accuracy by the fitted ABG + WL is given as an empirical benchmark. It can be seen that the local approach yields the best results for all scenarios. The global approach achieves slightly worse results with RMSE values. While the performance on the *empty hall scenario* improves slightly, the prediction accuracy on the *cave scenario* deteriorates by 0.51 dB. By excluding the latter from training, the RMSE increases to 3.17 dB. This is the worst performance achieved in cross-scenario evaluation over all scenarios, but still outperforms the empirical benchmark by 2.03 dB. By taking a closer look, it is revealed that for the transmitter position in the scenario's corner the RMSE amounts to 2.62 dB, whereas it is 3.66 dB for the transmitter position in the scenario's front. For all other scenarios, IndoorDRaGon scored RMSE values between 2.00 dB and 2.77 dB that are very similar for both transmitter positions. The fitted obstacle shadowing model achieves noticeably worse results, except for the *empty hall scenario*, as IndoorDRaGon is trained solely on scenarios with obstacles so that training and test data differ most here.

TABLE IV
Comparison of IndoorDRaGon's Prediction Accuracy

Scenario	IndoorDRaGon			Empirical Benchmark
	Local	Global	Cross	
Empty Hall	1.32 dB	1.30 dB	2.77 dB	2.30 dB
Hallway 1	1.47 dB	1.52 dB	2.14 dB	3.21 dB
Hallway 2	1.29 dB	1.52 dB	2.00 dB	2.96 dB
Diagonal	1.45 dB	1.60 dB	2.43 dB	3.15 dB
Cave	1.32 dB	1.83 dB	3.17 dB	5.20 dB
Bulk	1.46 dB	1.47 dB	2.52 dB	3.57 dB

Comparison of IndoorDRaGon's prediction accuracy as RMSE values for all scenarios and different data aggregation methods. The empirical benchmark here is the fitted ABG + WL.

Feature Importance: In order to gain insight into the impact of the different features on IndoorDRaGon's RF, we consider SHapley Additive exPlanations (SHAP) [20] in Fig. 9. Here, 80% of the aggregated and shuffled data is used for training. Grouping the features based on their logical feature domains (see Tab. II) reveals that $\mathbf{x}_{\text{pos}}$ features have the strongest impact on the model output. Particularly significant is Δy, which can be explained by the fact that this value represents a major part of the receiver-transmitter distance (cf. Fig. 4 (b)). Moreover, the $\mathbf{x}_{\text{top}}$ features are considered important. Especially the relation of obstacle pixels for split v_2. In general, low feature values result in higher model output here, while high feature values result in lower model output. For $\mathbf{x}_{\text{side}}$, the feature extracted from v_0 is considered the most important. It indicates whether there are obstacles directly in front of the receiver. In contrast to $\mathbf{x}_{\text{top}}$, low feature values lead to reduced model output. It can be seen that carrier frequency f, bandwidth B, and transmission power P_{TX} have no influence on the model output, as they do not vary across

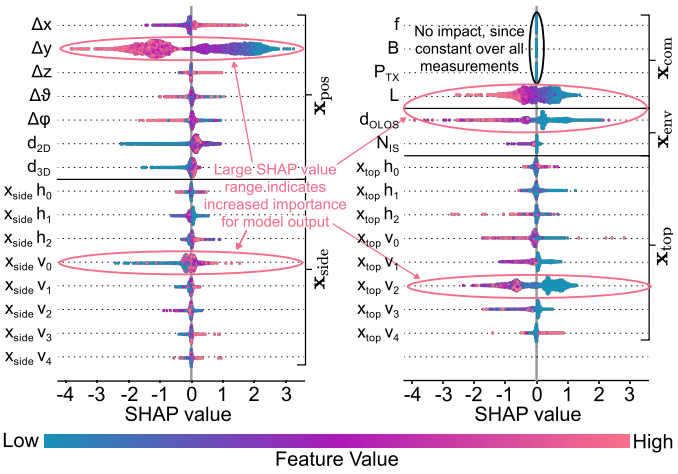

Fig. 9. SHAP feature impact on the model output of the globally trained RF sorted by logical feature domains (cf. Tab. II). See Fig. 3 (b) and (d) for an overview of the split sections of the image samples.

the measurements. In contrast, estimated path loss L affects the model output significantly, where high L reduces and low L increases the model output. In the $\mathbf{x}_{\text{env}}$ feature domain, d_{OLOS} is considered the most important feature.

In order to gain a deeper understanding of IndoorDRaGon's performance in the cross-scenario comparison, we also investigate the SHAP feature impact on the cross-scenario as well as on the local models. In terms of the latter, the feature importances are quite similar for all non-empty hall models. A noticeable difference is found between the non-empty hall models and the empty hall model, since $\mathbf{x}_{\text{env}}$ features are always zero and $\mathbf{x}_{\text{img}}$ only slightly differs. It is found that for all models the receiver-transmitter distance is remarkably meaningful, but some models take into account mostly the d_{3D} while other models focus on the Δy.

Comparing the cross-scenario feature importances for a reference scenario with those of the locally trained model reveals more significant differences, especially concerning the $\mathbf{x}_{\text{img}}$ features. Most significant differences between the cross-scenario and locally trained models are found for *empty hall scenario* and *cave scenario*, which explains its poor performance in cross-scenario evaluation.

VII. Conclusion

In this paper, we presented IndoorDRaGon as a novel ML-based path loss prediction method for dynamically changing 3D indoor environments. As demonstrated in a comprehensive performance evaluation campaign, IndoorDRaGon can effectively respond to dynamic changes in the environment not covered in the training process and allows to achieve more accurate prediction results than existing methods by implicitly incorporating scenario characteristics. That makes IndoorDRaGon a good candidate for network planning as well as arrangement planning for objects in dynamically changing environments.

In future works, we aim to further increase IndoorDRaGons generalizability by considering other indoor environments and analyzing IndoorDRaGons transferability. In this context, it can also be investigated to reduce the computational load by excluding the images from the entire process. In addition, we plan to utilize IndoorDRaGon in the context of machine learning-enabled network planning.

Acknowledgment

This work has been supported by the German Federal Ministry of Education and Research (BMBF) in the course of the *6GEM* research hub under grant no. 16KISK038 and by the Ministry of Economic Affairs, Industry, Climate Action and Energy of the State of North Rhine-Westphalia (MWIKE NRW) in the course of the project *Plan&Play* under grant no. 005-2008-0047, and in the course of the *5Guarantee* under grant no. 005–2008–0046.

References

[1] A. Rostami, "Private 5G Networks for Vertical Industries: Deployment and Operation Models," in *2019 IEEE 2nd 5G World Forum (5GWF)*, 2019, pp. 433–439.

[2] M. Wollschlaeger, T. Sauter, and J. Jasperneite, "The Future of Industrial Communication: Automation Networks in the Era of the Internet of Things and Industry 4.0," *IEEE Industrial Electronics Magazine*, vol. 11, no. 1, pp. 17–27, 2017.

[3] 3GPP, "study on communication for automation in vertical domains (CAV)," 3rd Generation Partnership Project (3GPP), Tech. Rep.

[4] B. Sliwa, M. Geis, C. Bektas, M. López, P. Mogensen, and C. Wietfeld, "DRaGon: Mining Latent Radio Channel Information from Geographical Data Leveraging Deep Learning," in *2022 IEEE Wireless Commun. and Networking Conf. (WCNC)*, 2022, pp. 2459–2464.

[5] M. Geis, B. Sliwa, C. Bektas, and C. Wietfeld, "TinyDRaGon: Lightweight Radio Channel Estimation for 6G Pervasive Intelligence," in *2022 IEEE Future Networks World Forum (FNWF)*, Montreal, Canada, Oct. 2022, Best Paper Award.

[6] H. T. Friis, "A Note on a Simple Transmission Formula," *Proceedings of the IRE*, vol. 34, no. 5, pp. 254–256, 1946.

[7] 3GPP, "5G; Study on channel model for frequencies from 0.5 to 100 GHz," 3rd Generation Partnership Project (3GPP), Technical Report (TR) 38.901, Apr 2022, version 17.0.0 Release 17.

[8] ITU, "Guidelines for evaluation of radio interface technologies for IMT-2020," Report, Oct 2017.

[9] Z. Yun and M. F. Iskander, "Ray tracing for radio propagation modeling: Principles and applications," *IEEE Access*, vol. 3, pp. 1089–1100, Jul 2015.

[10] S. Sun *et al.*, "Propagation path loss models for 5g urban micro- and macro-cellular scenarios," in *2016 IEEE 83rd Vehicular Technology Conf. (VTC Spring)*, 2016, pp. 1–6.

[11] P. Kyösti *et al.*, "WINNER II channel models," IST, Report, Sep 2007.

[12] ITU, "Effects of building materials and structures on radiowave propagation above about 100 MHz," Report, Sep 2021.

[13] K. Preusser, P. Lölver, M. Garling, and A. Schmeink, "Indoor Factory RSRP and RTT Measurements at 3.7 GHz: Simulator and Analysis," in *2022 5th Int. Conf. on Advanced Commun. Technologies and Networking (CommNet)*, Dec. 2022, pp. 1–8.

[14] H. Cheng, H. Lee, and S. Ma, "CNN-Based Indoor Path Loss Modeling with Reconstruction of Input Images," in *2018 Int. Conf. on Inf. and Commun. Technology Convergence (ICTC)*, 2018, pp. 605–610.

[15] X. Cai, G. Zhang, C. Zhang, W. Fan, J. Li, and G. F. Pedersen, "Dynamic Channel Modeling for Indoor Millimeter-Wave Propagation Channels Based on Measurements," *IEEE Transactions on Commun.*, vol. 68, no. 9, pp. 5878–5891, 2020.

[16] L. Breiman, "Random Forests," *Mach. Learn.*, vol. 45, no. 1, pp. 5–32, Oct 2001.

[17] Innovationlab. (2017) Innovationlab Hybrid Services in Logistics. [Online]. Available: https://www.innovationlab-logistics.com/research-centre/

[18] 3GPP, "5G; NR, Physical layer measurements," 3rd Generation Partnership Project (3GPP), Technical Specification (TS) 38.215, Jul 2020, version 16.2.0 Release 16.

[19] ——, "5G; NR, Base Station (BS) radio transmission and reception," 3rd Generation Partnership Project (3GPP), Technical Specification (TS) 38.104, Jul 2020, version 16.4.0 Release 16.

[20] S. M. Lundberg and S.-I. Lee, "A unified approach to interpreting model predictions," in *Proceedings of the 31st Int. Conf. on Neural Inf. Processing Systems*, ser. NIPS'17. Red Hook, NY, USA: Curran Associates Inc., 2017, p. 47684777.